Electronic Supplementary Material (ESI) for Journal of Materials Chemistry C.
This journal is © The Royal Society of Chemistry 2022

Supporting Information Section

Mechanistic Insights into Supersaturation mediated Large Area Growth of hexagonal Boron Nitride for Graphene Electronics

*Ankit Rao, Srinivasan Raghavan**

Centre for Nano Science and Engineering, Indian Institute of Science, Bengaluru 560012

*E-mail: sraghavan@iisc.ac.in

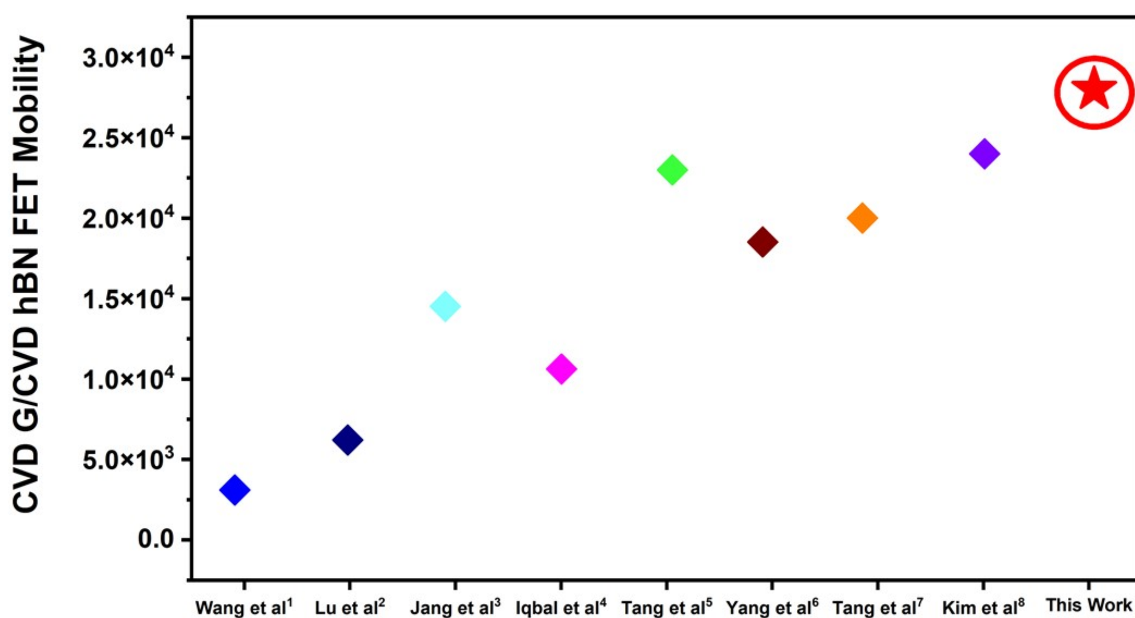

Figure S1. Comparison of FET Mobility values of CVD Graphene on CVD hBN[1–8]

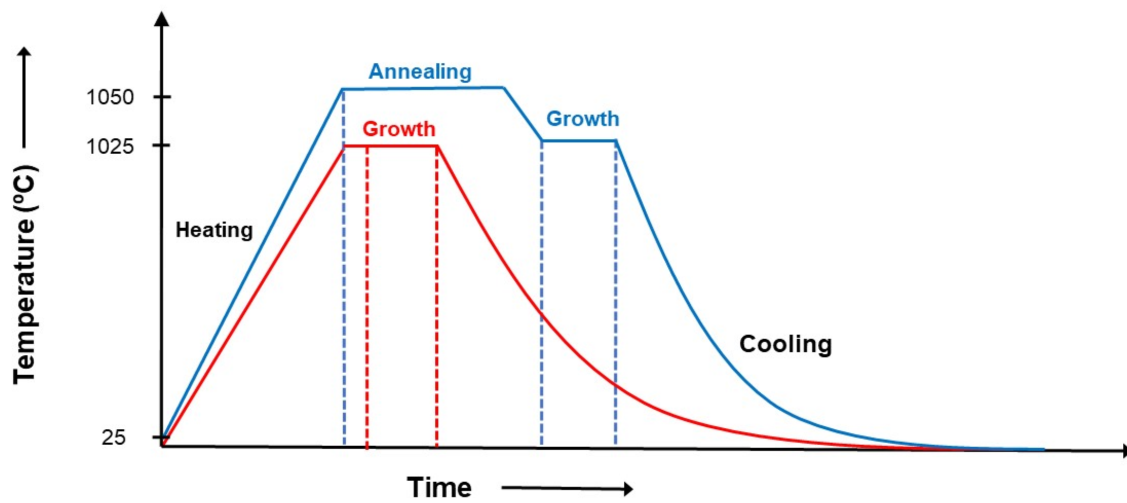

Figure S2. Schematic of the temperature profile for the growth setup for controlled h-BN growth.

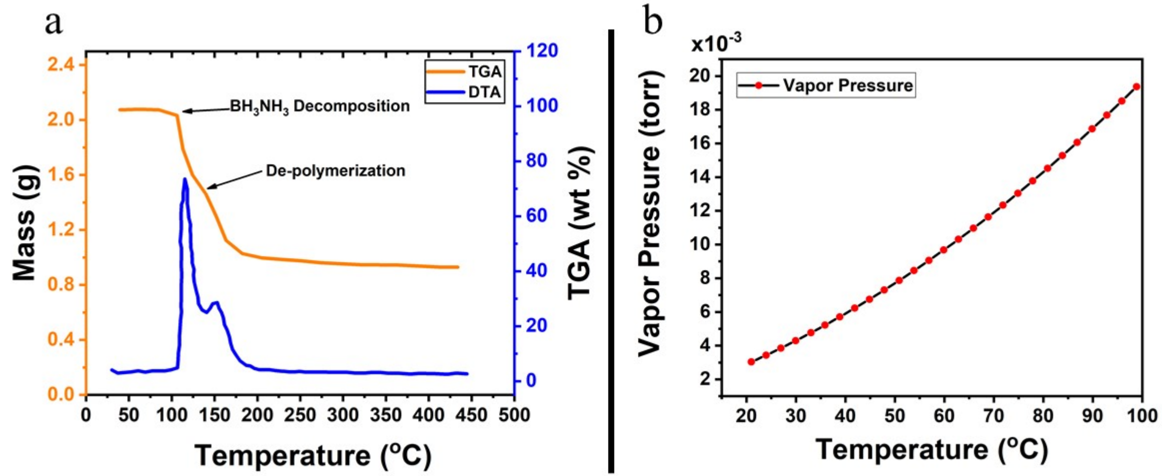

Figure S3. a) TGA/DTA curve of BH3NH3 for a temperature range from 25C to 450C. b) Vapor pressure plot of BH3NH3 in torr.

The precursor flux is a function of vapor pressure of the precursor (P_{BH3NH3}), the flow rate of the carrier gas ($\eta_{carrier}$) and the pressure maintained inside the vaporizer setup ($p_{vaporizer}$) as given in eqn (S4).

$$p_{BH_3NH_3} = \left[\left(\frac{dm}{dt}\right)\sqrt{\frac{T}{M}}\right] \quad \text{(S1)}$$

$$\eta_{BH_3NH_3} = \frac{p_{BH_3NH_3} * \eta_{carrier}}{p_{vaporizer}} \quad \text{(S2)}$$

where dm/dt is the rate of mass loss obtained from TGA/DTA plot, T is the temperature in kelvins, M is the molecular weight of the precursor and R is the gas constant.

S1. Nanocrystalline Boron Nitride

The amount of n-BN by-product and the reactivity on the surface increases with increase in partial pressure as shown in Fig S4a. The decrease in carrier flow rate results in lesser amount of hydrogen reacting with the precursor reactor and hence results in reduction of n-BN density. This allows us to obtain clean h-BN which is an essential factor for its application as a substrate.

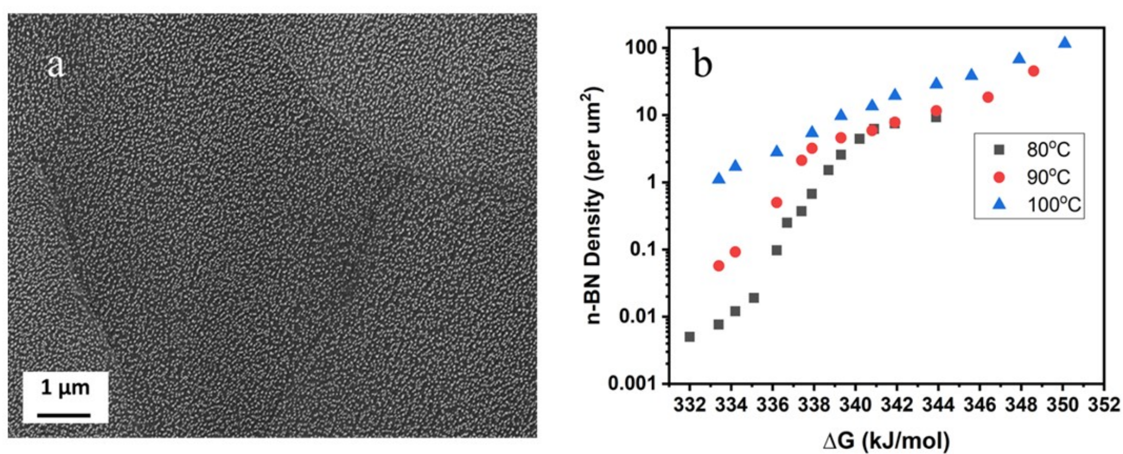

Figure S4. a) n-BN particles covering the Cu surface. b) Experimental n-BN density as a function of supersaturation.

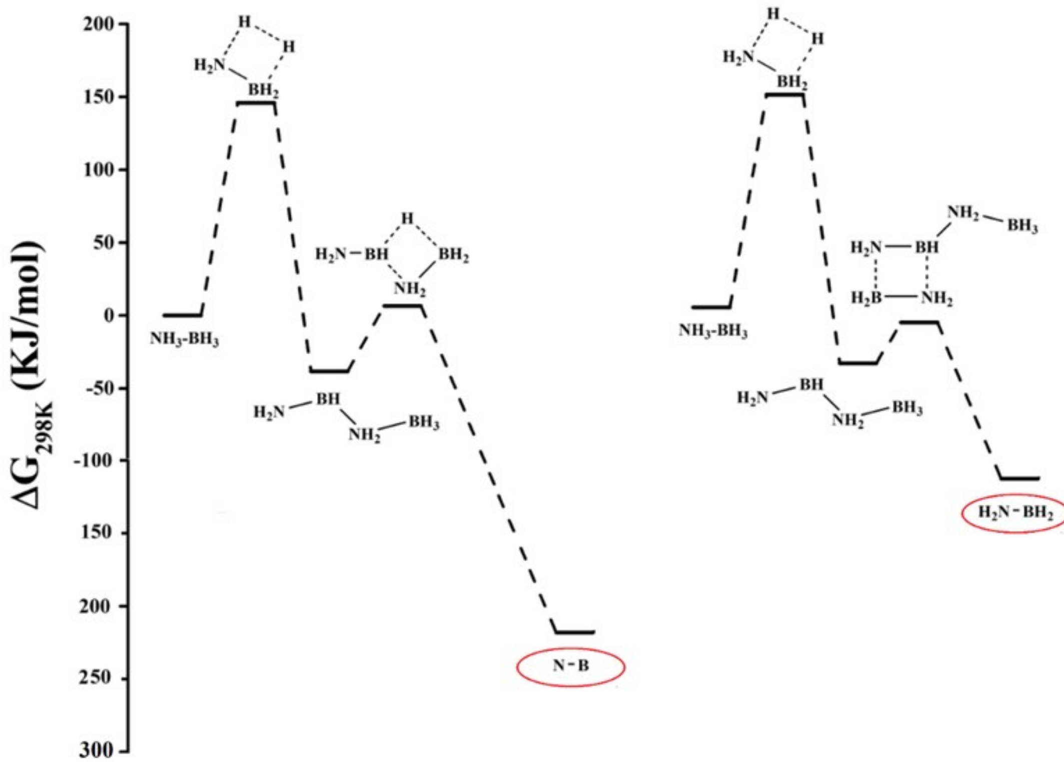

Figure S5. Potential Energy Surface diagram for the formation of h-BN and BNH_4 from BH_3-NH_3[9].

$$n(BH_3NH_3) \rightarrow (BH_2NH_2)_n + nH_2 \qquad -(S3) \quad \Delta G^o = -152.7\ kJ/mol$$

$$BH_3NH_3 \rightarrow hBN + 3H_2 \qquad -(S4) \quad \Delta G^o = -343.4\ kJ/mol$$

Eqn (S5) is derived from the supersaturation equation to calculate the equilibrium partial pressure of the precursor as a function of temperature and total reactor pressure. This value indicates the minimum partial pressure of the precursor required for the formation of hBN on the surface of Cu.

$$p^{eq}_{BH_3NH_3} = \frac{P_{total}}{1 + \frac{e^{\left(\frac{-\Delta G^o}{RT}\right)}}{P^2_{total}}} \qquad \text{(S5)}$$

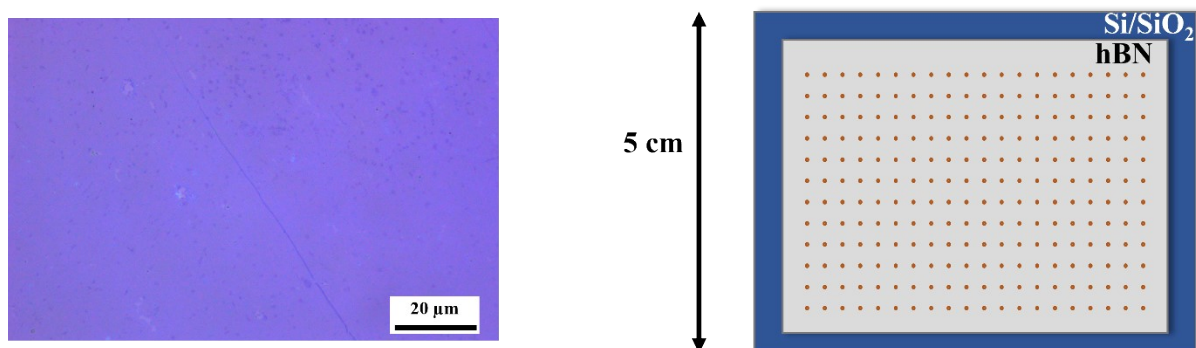

Figure S6. (a) Optical image of the transferred multilayer (5 layer) thick hBN. b) Raman mapping measurements on 25 cm2 area hBN transferred onto Si/SiO2.

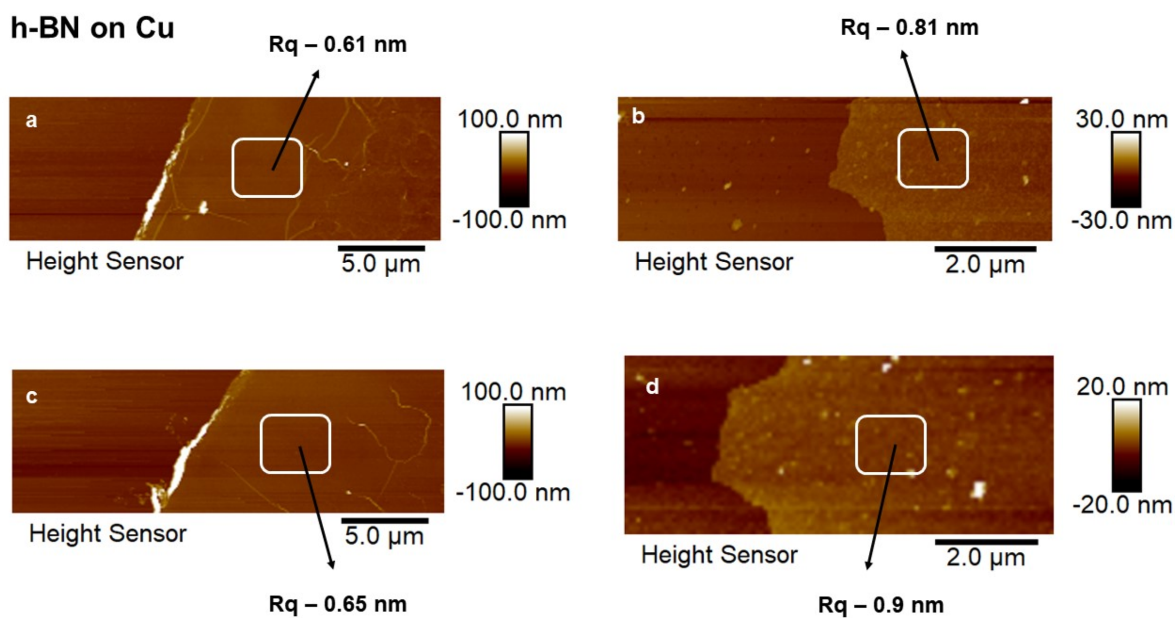

Figure S7. AFM scans with roughness Rq of films grown on Cu. a) On 28nm film grown on Cu, b) 5nm film grown on Cu, c) 28 nm film transferred on Si/SiO_2, d) 5 nm film transferred on Si/SiO_2

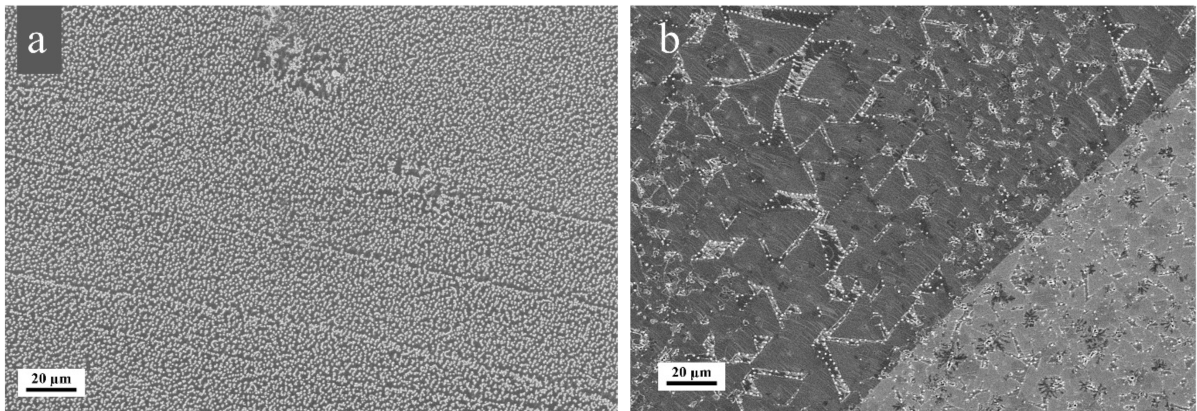

Figure S8. SEM image of h-BN grown on (a) unannealed Cu substrate and (b) annealed Cu substrate at exact conditions exhibiting the effect on substrate morphology on growth.

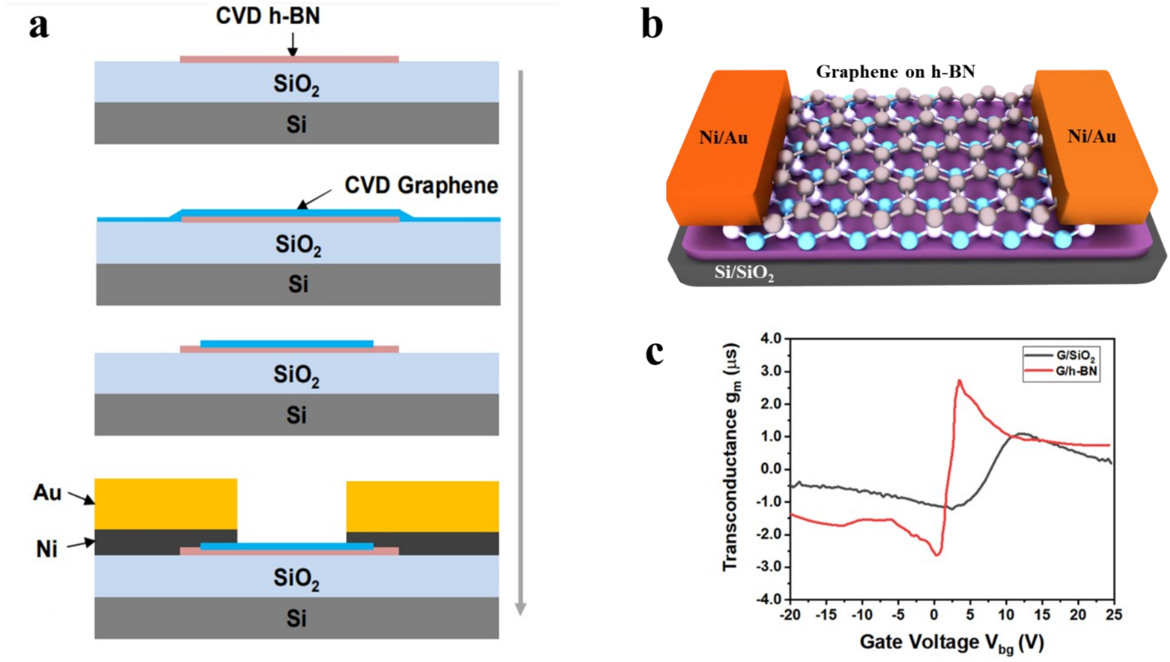

Figure S9. a) Process flow for fabrication of G/h-BN devices, b) Schematic of the fax`bricated device. c) Transconductance (gm) vs Gate Voltage (Vg) of the fabricated device.

S2. Mobility Extraction

In the transconductance method or the Drude model, gate voltage dependent transconductance is used to calculate the field effect mobility, i.e.

$$\mu_{FET} = g_m \frac{L}{W V_{ds} C_{ox}} \quad \text{(S5)}$$

where $g_m = \frac{\partial I_d}{\partial V_g}$ is transconductance and the mobility μ_{FET} is the field-effect mobility. Due to the ignorance of contact resistance, field-effect mobility is always lower than the real mobility at any given gate voltage, and the gap between field-effect mobility and actual value depends on gate voltage, channel length and conduction type.

While the choice of the model to extract mobility varies widely in the literature, Ruoff et. al.[10] showed that the constant mobility fit is the most physically apt one. The constant mobility fit model fits the observed channel resistance variation with the gate voltage very nicely over entire range. Hence, in this work, the constant mobility fit is the method used to extract the mobility along with the transconductance method.

Furnace Temperature (°C)	Reactor Pressure (torr)	Reactor Pressure (atm)	BH3-NH3 Flow Rate (Calculated)	Ar Flow Rate (sccm)	H2 Flow Rate (sccm)	H2 Flow Rate (bubbler)	Eqm Partial Pressure (BH3NH3)	Partial Pressure (BH3NH3)	ΔG (kJ/mol)
950	3	0.0039	0.0085	500	10	1	1.074E-10	6.36E-07	297.718
950	1.9	0.0025	0.0107	200	30	10	1.203E-10	1.07E-06	317.023
975	0.5	0.0007	0.0012	50	20	10	1.017E-09	1.10E-07	311.203
975	2.2	0.0029	0.0128	400	20	1	1.756E-10	8.42E-07	298.094
1000	0.5	0.0007	0.0026	50	20	1	8.586E-11	2.31E-07	303.876
1000	3	0.0039	0.0128	500	20	10	2.41E-10	9.36E-06	298.570
1000	0.5	0.0007	0.0070	50	20	1	7.017E-10	6.14E-07	295.305
1020	0.5	0.0007	0.0064	50	20	10	1.017E-09	5.61E-07	294.827
1020	2.2	0.0029	0.0107	300	20	1	3.811E-10	9.08E-07	302.440
1025	0.5	0.0007	0.0014	50	20	1	9.108E-09	1.80E-07	306.410
1025	1.2	0.0016	0.0040	150	10	1	1.449E-10	3.68E-07	292.231
1025	3.8	0.0050	0.0085	750	30	10	2.945E-10	5.33E-07	305.079
1025	10	0.0007	0.0140	50	20	10	6.449E-09	1.15E-06	290.532
1025	1.2	0.0016	0.0049	100	30	1	1.407E-08	5.13E-07	322.372
1025	1.5	0.0020	0.0049	50	10	10	1.73E-09	1.37E-06	313.973
1025	0.9	0.0012	0.0020	50	50	10	2.051E-10	2.41E-07	336.026
1025	5	0.0066	0.0085	500	30	10	2.064E-09	1.02E-06	319.089
1025	5	0.0066	0.0078	100	30	1	4.018E-07	9.42E-06	348.102
1030	0.5	0.0007	0.0009	50	20	10	7.109E-10	7.91E-07	311.462
1030	0.5	0.0007	0.0010	40	30	1	2.262E-09	9.52E-07	321.995
1030	1	0.0013	0.0008	50	20	10	5.46E-11	1.83E-07	327.119
1030	10	0.0013	0.0008	50	20	1	5.46E-09	1.43E-07	327.119
1030	1	0.0013	0.0005	50	40	10	1.978E-10	7.44E-07	348.157
1040	0.5	0.0007	0.0009	50	20	1	7.111E-10	7.91E-07	310.882
1040	1	0.0013	0.0008	100	20	1	1.096E-09	8.38E-07	314.969
1040	0.5	0.0007	0.0010	40	30	10	2.263E-10	9.52E-07	321.496
1040	1	0.0013	0.0008	50	20	10	5.462E-09	1.53E-07	326.659
1040	1	0.0013	0.0005	50	40	1	1.979E-10	7.44E-07	347.859

1050	0.5	0.0007	0.0009	100	20	10	7.144E-09	4.64E-07	298.574
1050	0.5	0.0007	0.0010	40	30	1	2.263E-10	9.52E-07	320.997
1050	1	0.0013	0.0005	100	40	10	5.295E-10	4.79E-07	337.893
1050	1	0.0013	0.0008	50	20	1	5.463E-09	1.43E-07	326.199
1050	1	0.0013	0.0008	50	40	10	1.979E-09	1.12E-07	343.100

Table S1. A summary of the growth conditions at various growth conditions to study the effect of supersaturation

Run No.	Furnace Temperature (°C)	Reactor Pressure (torr)	BH3-NH3 Flow Rate (Calculated)	Ar Flow Rate (sccm)	H2 Flow Rate (sccm)	Vapor Pressures (BH3NH3)	Supersaturation (kJ/mol)
1	1025	10	0.0085	100	30	0.00528	362.092
2	1025	1	0.0005	50	40	0.0128	348.157
3	1025	1	0.0005	50	40	0.0128	348.157
4	1025	1	0.0026	50	50	0.0128	335.779
5	1025	2	0.0107	200	80	0.0128	332.428
6	1025	5	0.0085	300	30	0.0128	328.845
7	1025	1	0.0008	50	20	0.0128	327.119
8	1025	0.5	0.0010	40	30	0.0128	321.995
9	1025	5	0.0085	500	30	0.0128	319.089
10	1025	5	0.0085	700	30	0.0128	312.395
11	1025	0.5	0.0016	50	20	0.0128	314.579
12	1025	0.5	0.0009	50	20	0.0128	311.462
13	1025	3	0.0085	500	30	0.0128	308.064
14	1025	3	0.0085	500	30	0.0128	308.064
15	1025	5	0.0085	900	30	0.0128	307.293
16	1025	5	0.0085	900	30	0.0128	307.293
17	1025	3	0.0160	500	30	0.0128	306.794
18	1025	3	0.0071	600	30	0.0128	306.426
19	1025	0.5	0.0026	50	20	0.0128	301.915
20	1025	3	0.0128	500	20	0.0128	296.860
21	1025	3	0.0085	500	10	0.0128	292.326
22	1025	0.5	0.0064	50	20	0.0128	294.113
23	1025	0.5	0.0064	50	20	0.0128	294.113

Table S2. A summary of the growth conditions at 1025°C

No.	Furnace Temperature	Reactor Pressure (torr)	BH3-NH3 Flow Rate (Calculated)	Ar Flow Rate	H2 Flow Rate	H2 Flow Rate (bubbler)	Time (min)	Partial Pressure (BH3NH3)	Partial Pressure (H2)	Supersaturation
1	1025	3	8.53E-03	500	30	20	10	6.12E-08	1.64E-01	308.06
2	1025	3	8.53E-03	500	30	20	15	6.12E-08	1.64E-01	308.06
3	1025	3	8.53E-03	500	10	20	10	6.36E-08	5.66E-02	292.33
4	1025	4.3	8.53E-03	500	30	20	15	8.78E-08	2.35E-01	315.83
5	1025	5	8.53E-03	500	30	20	15	1.02E-07	2.73E-01	319.09
6	1025	3	1.28E-02	500	20	20	30	9.36E-08	1.11E-01	296.86
7	1025	3	1.60E-02	500	30	30	30	1.13E-07	1.61E-01	306.79
8	1025	5	8.53E-03	300	30	20	15	1.60E-07	4.29E-01	328.84
9	1025	2.2	1.07E-02	300	20	20	25	9.08E-08	1.29E-01	302.12
10	1025	10	2.48E-02	250	50	20	5	1.02E-06	1.56E+00	345.12
11	1025	1.9	8.53E-03	250	30	20	25	7.11E-08	1.90E-01	311.29
12	1025	2	1.07E-02	200	80	20	15	9.36E-08	5.33E-01	332.43
13	1025	2.2	8.53E-03	200	100	20	40	7.72E-08	6.88E-01	341.4
14	1025	1.9	1.07E-02	200	30	20	40	1.07E-07	2.28E-01	312.82
15	1025	10	1.17E-02	150	30	20	10	7.70E-07	1.50E+00	352.48
16	1025	3.5	4.56E-03	150	30	20	7	1.05E-07	5.25E-01	339.99
17	1025	1.2	3.97E-03	150	10	10	10	3.68E-08	7.06E-02	292.23
18	1030	1.5	4.00E-02	150	30	20	20	3.95E-07	2.25E-01	299.34
19	1030	1.2	4.00E-02	150	30	20	30	3.16E-07	1.80E-01	294.5
20	1025	1.2	4.88E-03	100	30	20	10	5.13E-08	2.40E-01	322.37
21	1025	5	7.80E-03	100	30	20	7	3.42E-07	1.00E+00	348.1
22	1025	10	8.53E-03	100	30	20	15	7.49E-07	2.00E+00	362.09
23	1030	1.2	1.71E-03	100	50	1	30	1.78E-08	3.97E-01	335.41
24	1000	5	7.93E-03	50	50	20	5	4.35E-07	2.08E+00	358.89
25	1025	1.5	4.88E-03	50	10	10	5	1.37E-07	2.14E-01	313.97
26	1030	0.5	6.40E-03	50	20	5	30	5.61E-08	1.33E-01	294.11
27	1030	0.5	2.56E-03	50	20	3	30	2.31E-08	1.37E-01	301.92
28	1030	0.5	6.40E-04	50	20	1	30	5.93E-09	1.41E-01	314.58
29	1030	1	7.68E-04	50	20	0.6	30	1.43E-08	2.83E-01	327.12
30	1030	1	5.12E-04	50	40	0.6	25	7.44E-09	4.42E-01	348.16
31	1030	1	2.56E-03	50	50	1	30	3.34E-08	4.95E-01	335.78
32	1030	0.9	2.05E-03	50	50	0.8	20	2.41E-08	4.46E-01	335.83

Table S3. Set of growth runs indicating the effects of H_2 partial pressure with other parameters being constant.

References

1. Wang, M. *et al.* A platform for large-scale graphene electronics - CVD growth of single-layer graphene on CVD-grown hexagonal boron nitride. *Adv. Mater.* **25**, 2746–2752 (2013).

2. Lu, G. *et al.* Synthesis of large single-crystal hexagonal boron nitride grains on Cu-Ni alloy. *Nat. Commun.* **6**, 1–7 (2015).

3. Jang, A. R. *et al.* Wafer-Scale and Wrinkle-Free Epitaxial Growth of Single-Orientated Multilayer Hexagonal Boron Nitride on Sapphire. *Nano Lett.* **16**, 3360–3366 (2016).

4. Iqbal, M. W., Iqbal, M. Z., Jin, X., Eom, J. & Hwang, C. Superior characteristics of graphene field effect transistor enclosed by chemical-vapor-deposition-grown hexagonal boron nitride. *J. Mater. Chem. C* **2**, 7776–7784 (2014).

5. Tang, S. *et al.* Silane-catalysed fast growth of large single-crystalline graphene on hexagonal boron nitride. *Nat. Commun.* **6**, 6499 (2015).

6. Yang, W. *et al.* Epitaxial growth of single-domain graphene on hexagonal boron nitride. *Nat. Mater.* **12**, 792–797 (2013).

7. Tang, S. *et al.* Precisely aligned graphene grown on hexagonal boron nitride by catalyst free chemical vapor deposition. *Sci. Rep.* **3**, 2666 (2013).

8. Kim, E., Jain, N., Jacobs-Gedrim, R., Xu, Y. & Yu, B. Exploring carrier transport phenomena in a CVD-assembled graphene FET on hexagonal boron nitride. *Nanotechnology* **23**, 125706 (2012).

9. Kumar, V., Roy, B. & Sharma, P. Kinetics of borazine formation from ammonia borane dehydrocoupling reaction through Ab initio analysis. *Int. J. Hydrogen Energy* **44**, 22022–22031 (2019).

10. Venugopal, A., Chan, J., Li, X., Magnuson, C. W., Kirk, W. P., Colombo, L., Ruoff, R., & Vogel, E. M. Effective mobility of single-layer graphene transistors as a function of channel dimensions. Journal of Applied Physics, **109**(10), 104511, (2011).